Carbohydrate Polymers 86 (2011) 1038–1047

Contents lists available at ScienceDirect

Carbohydrate Polymers

journal homepage: www.elsevier.com/locate/carbpol

Binding interactions of α-amylase with starch granules: The influence of supramolecular structure and surface area

Frederick J. Warren[a], Paul G. Royall[b], Simon Gaisford[c], Peter J. Butterworth[a], Peter R. Ellis[a,*]

[a] King's College London, Diabetes and Nutritional Sciences Division, Biopolymers Group, Franklin-Wilkins Building, 150 Stamford Street, London SE1 9NH, United Kingdom
[b] King's College London, Institute of Pharmaceutical Science, Drug Delivery Group, Franklin-Wilkins Building, 150 Stamford Street, London SE1 9NH, United Kingdom
[c] University of London, School of Pharmacy, 29-39 Brunswick Square, London WC1N 1AX, United Kingdom

ARTICLE INFO

Article history:
Received 8 April 2011
Received in revised form 25 May 2011
Accepted 26 May 2011
Available online 24 June 2011

Keywords:
Starch
α-Amylase
Binding kinetics
DSC
FTIR–ATR
Particle sizing

ABSTRACT

Factors affecting the α-amylase-catalysed hydrolysis kinetics of starch are incompletely understood, but are of importance to postprandial metabolism and many industrial processes (e.g. bioethanol production). Also, reports on the role of surface area and amorphous content in influencing amylolysis are conflicting. Binding kinetics of pancreatic α-amylase with native starch granules at 0 °C were compared with information on starch characteristics. Dissociation constants (K_d), obtained for amylase binding to starches of different particle sizes by solution-depletion assay, varied from 0.16 to 2.05 mg/mL. K_d was strongly dependent on specific surface area of the starch granules. Binding rates of amylase (4 nM concentration) to the starch were calculated from the time-dependency of amylase depletion and ranged from 1.95 to 22.04×10^{-3} s^{-1}. The rates were strongly dependent on the degree of order of α-glucan chains of starch, as measured by DSC and FTIR–ATR. Thus, α-amylase binds most readily to exposed/available amorphous α-glucan chains.

1. Introduction

Insight into the physical and chemical characteristics of starch that influence the rate at which it is hydrolysed is of importance in the fields of digestive physiology, gut hormone signalling and postprandial metabolism, since starch forms a major part of the exogenous, 'digestible' carbohydrate supply in the human diet (Butterworth, Ellis, & Roder, 2005). Thus, the rate and extent of starch digestion play a crucial role in regulating the rise in postprandial blood glucose and insulin concentrations (Ells, Seal, Kettlitz, Bal, & Mathers, 2005; Mann, 2007). Attenuating the fluctuations in postprandial glycaemia and insulinaemia has implications for health, particularly in relation to the prevention and treatment of diabetes mellitus (Mann, 2007). Also, in the field of animal feeds science, maximising yields by utilising botanical varieties of starch and processing conditions which optimise the energy that livestock obtain from their feeds, is important for farm economics (Svihus, Uhlen, & Harstad, 2005). Moreover, starch hydrolysis is a key step in certain industrial processes, such as brewing, and the production of high glucose syrups and bioethanol (Robertson et al., 2005; Tester, Qi, & Karkalas, 2006). In such industrial settings, an improved understanding of the mechanism of starch hydrolysis can reduce production costs and energy usage by improving efficiency. However, despite a large body of published work on this topic, there is still much uncertainty in the literature as to the mechanism(s) by which the structural characteristics of starch granules influence the interaction of amylase with starch and subsequent amylolysis (Dhital, Shrestha, & Gidley, 2010; Tahir, Ellis, & Butterworth, 2010; Tahir, Ellis, Bogracheva, Meares-Taylor, & Butterworth, 2011).

Starch is the main storage carbohydrate in all higher plants and is comprised of two anhydroglucose polymers, amylose and amylopectin. These two α-glucan polymers are organised into a complex, semi-crystalline granular structure, with a particle size ranging from 1 to 100 μm in diameter. The structure of the starch granule has been extensively reviewed elsewhere (Robyt, 2008; Wang, Bogracheva, & Hedley, 1998). Since native starch is in a granular form, its hydrolysis kinetics are complicated by the necessity for the enzyme to diffuse towards and adsorb onto the granule surface before the catalytic step can proceed (Slaughter, Ellis, & Butterworth, 2001). The adsorption and binding of the enzyme to the granule surface is, therefore, a key step in starch hydrolysis. The starch granule (0.5–50 μm radius) is many times greater in size than the hydrolytic enzyme (~4 nm hydrodynamic radius; Boistelle, Astier, Marchis-Mouren, Desseaux, & Haser, 1992). The adsorption of an enzyme onto a solid substrate is dependent on the

* Corresponding author at: Biopolymers Group, Diabetes and Nutritional Sciences Division, King's College London, Franklin-Wilkins Building (Room 4.102), 150 Stamford Street, London SE1 9NH, UK. Tel.: +44 0 207 848 4238; fax: +44 0 207 848 4171.
E-mail address: peter.r.ellis@kcl.ac.uk (P.R. Ellis).

0144-8617/$ – see front matter © 2011 Elsevier Ltd. All rights reserved.
doi:10.1016/j.carbpol.2011.05.062

number and accessibility of available binding sites (Mclaren, 1963). The primary factors that may affect adsorption specifically to starch include the particle size (and therefore exposed surface area) of the granule, the presence of pores/crevices in the granule surface and the supramolecular structure of the carbohydrate chains at exposed surfaces of the granule (especially the relative proportions of amorphous and ordered α-glucan chains) (Colonna, Leloup, & Buleon, 1992; Slaughter et al., 2001; Tahir et al., 2010, 2011). The presence of non-carbohydrate components (i.e. lipid and protein) may also influence the interaction between α-amylase and the starch granule surface, but we believe such interactions are likely to be relatively unimportant, compared with the structural order of α-glucan chains at the enzyme–starch interface (Tahir et al., 2010, 2011).

Studies of adsorption of α-amylase to laboratory-manufactured starch crystallites revealed a specific, reversible process, which can be competitively inhibited by the presence of maltose and maltotriose (Colonna et al., 1992; Leloup, Colonna, & Ring, 1991). Although useful, this work was carried out on artificial crystallites created from low molecular weight linear glucose polymers. The crystallites possessed a mono-disperse size distribution and a very high degree of crystallinity, and so we believe that the work shed somewhat limited light on the aspects of starch structure that affect adsorption of α-amylase. The adsorption of barley malt α-amylase to starches has been studied using different varieties of native starches (Schwimmer & Balls, 1949) and fractionated large and small barley starch granules (MacGregor, 1979). These studies suggest that the particle size, and therefore available surface area, may be an important determinant of the binding efficiency of the enzyme to the starch granule. Previous experiments, however, suffered from the insensitivity of the assays used to detect the enzyme, necessitating the use of high enzyme concentrations. This led to the use of very short incubation periods (Schwimmer & Balls, 1949) and the likelihood of significant granule hydrolysis during the time course of the experiment (MacGregor, 1979). There was no certainty, therefore, that their binding systems had reached equilibrium, nor was it possible to exclude the occurrence of some starch digestion in spite of the short incubation periods.

The effectiveness of adsorption of the enzyme would be expected to be reflected in the rate of enzyme-catalysed starch hydrolysis, with smaller granules being hydrolysed at a greater rate than larger ones. A number of studies have compared hydrolysis rates to particle size, with mixed results. Some have shown a link between particle size and hydrolysis rates of both naturally occurring particle size distributions (Byoung-Wook, Jung-In, Myo-Jeong, & Jae, 2003; Tahir et al., 2010) and laboratory fractionated starches (Dhital et al., 2010; Knutson, Khoo, Cluskey, & Inglett, 1982; Manelius, Qin, Åvall, Andtfolk, & Bertoft, 1997; Sakintuna, Budak, Dik, Yondem-Makascioglu, & Kincal, 2003; Vasanthan & Bhatty, 1996) over a range of hydrolysis times, from minutes to days. This would seem to indicate that particle size plays an important role in amylolysis that is likely to be due to size effects on enzyme binding. There are, however, a number of conflicting reports suggesting that particle size has no effect on hydrolysis rate (Planchot, Colonna, Gallant, & Bouchet, 1995; Valetudie, Colonna, Bouchet, & Gallant, 1993; Zhang & Oates, 1999). The relationship of particle size to the interaction of α-amylase with the starch granule therefore clearly merits further investigation.

This paper reports on equilibrium binding kinetics for the interactions of α-amylase with a controlled sized range of starch granules, both naturally occurring and laboratory fractionated, and on investigations of the impact of the supramolecular structure and particle size of starch on the rate of enzyme binding. We have used a very sensitive fluorometric amylase assay with low enzyme concentrations so as to minimise amylolysis during the time course of the experiment (Egan, 2008). The relative proportions of ordered and amorphous carbohydrate structures in starch granules was assessed by differential scanning calorimetry (DSC) and Fourier transform infrared spectroscopy with attenuated total reflectance (FTIR–ATR). The ratio of ordered to disordered material can vary markedly between different botanical origins of starch, which in turn can have significant effects on starch properties (Tan, Flanagan, Halley, Whittaker, & Gidley, 2007). DSC provides a measure of the bulk ordered structure, while FTIR–ATR measures the degree of ordered structure at the surface of the starch granule.

2. Materials and methods

Except where specified, all chemicals were obtained from Sigma–Aldrich Chemical Company (Poole, Dorset, UK) and were of the highest available grade.

2.1. Sources, preparation and characterisation of starches

Wheat starch (Cerestar, cv. GL04) and pea starches (WT, *r* and *lam*; see Wang et al., 1998) were gifts from Prof. T. Bogracheva and Prof. C. Hedley (formerly of the John Innes Centre, Norwich, UK). WT pea starch is a wild type pea starch comprising of ~30% amylose and 70% amylopectin (dry w/w). The *r* mutant pea starch has a mutation at the *rugosa* gene locus, which results in a starch with a very high (~70%) amylose content, because of a decreased activity of granule-bound starch synthase 1 (Lloyd, Hedley, Bull, & Ring, 1996). The *lam* mutant starch has a mutation at the *low amylose* gene locus, and contains only ~10% amylose (Tahir et al., 2010, 2011; Wang et al., 1998). Potato starch was obtained from National Starch and Chemicals (UK). Waxy rice starch (cv. Remyrise) was a gift from Dr. P. Rayment (Unilever, UK), and is essentially free of amylose. Normal maize starch (cv. Globzeta) was a gift from Prof. I. Rowland (University of Reading, UK). The starches used in this study, including size fractionated samples (see below), have very low levels of impurities. As previously reported (Tahir et al., 2010), lipid and protein contents of the same batches of starch samples from different botanical sources were found to be ≤0.40% (w/w) and 0.31% (w/w), respectively, except *r* mutant pea starch which has a slightly higher level of 0.67% for protein. Size fractionated samples for wheat and potato were found to contain the same levels of impurities (e.g. protein) as the respective parent samples. Hence any differences in non-starch components between the various starches were negligible. Starch damage values for all samples, as determined by Congo red dye exclusion and microscopy, were found to be <0.5% of the total starch content (Slaughter et al., 2001).

2.2. Particle fractionation of starch granules

Wheat starch possesses a bimodal particle size distribution (e.g. Kim & Huber, 2008), which can be separated into its two component fractions using density centrifugation. This was carried out using a modification of the method of Kim and Huber (2008). A sample of 2.5 g of native wheat starch was suspended in 25 mL of 80% (w/v) sucrose (BDH AnalaR grade sucrose in dH_2O (deionised water) in a 50 mL conical Falcon tube), and thoroughly mixed (2 min whirly mixer, followed by inverting for 5 min). This was then spun in a bench top centrifuge (MSE Mistral 3000 fitted with a swing-out rotor) for 2 min at 310 × *g* (with no braking). The supernatant was removed to a beaker and the pellet thoroughly re-suspended in 25 mL of 80% (w/v) sucrose. The centrifugation step was then repeated 5 times. The final pellet consisted of the large granule fraction (defined as the A type granules) and was washed in dH_2O three times, followed by a single wash in absolute ethanol (BDH AnalaR grade 99.7–100% (v/v) purity), before being recovered by filtration on filter paper (Whatman hardened 50). The supernatants collected after each centrifugation step were pooled and then spun

for 30 min at 630 × g. The final supernatant was discarded and the pellets were washed 3 times in dH_2O, then once in absolute ethanol, before being recovered by filtration. This granule fraction consisted of the small granule fraction (defined as the B type granules).

Potato starch has a very broad particle size distribution, and this was exploited to create two granule fractions of different sizes, using a further modification of the method of Kim and Huber (2008). A 2.5 g sample of native potato starch was suspended in 25 mL of 80% (w/v) sucrose in a 50 mL conical Falcon tube, and thoroughly mixed. This was then spun for 1 min at 15 × g with no braking. The supernatant was removed to a beaker, and the pellet thoroughly re-suspended in 25 mL of 80% (w/v) sucrose. The centrifugation step was then repeated 5 times. The final pellet consisted of the large granule fraction, and was washed in dH_2O three times, followed by a single wash in absolute ethanol, before being recovered by filtration on filter paper. The pooled supernatants from each centrifugation step were then spun for 2 min at 50 × g, and the final supernatant was discarded. The remaining pellet, comprised of the smaller size fraction, was washed 3 times in dH_2O, followed by a single wash in absolute ethanol, before being recovered by filtration. All the particle size fractions were then equilibrated at atmospheric humidity (which is kept relatively constant in the laboratory at 55–60% relative humidity).

2.3. Particle size analysis

Particle size analysis was carried out for all starches using a Beckman Coulter Multisizer 3® Coulter Counter fitted with either a 100 or 140 μm orifice tube, depending on the size of the fraction being tested. A small amount (≈1 mg) of the native starch was dispersed in ≈200 mL of 0.9% saline (Fresenius Kabi, Steriflex®). A 2 mL volume was used for analysis. The instrument was calibrated with Coulter Counter standard L10 polystyrene latex (mode diameter 9.92 μm). Data were analysed according to Tahir et al. (2010). Specific surface area (SSA) was calculated from median (d_{50}) particle size diameters using the following equation:

$$\mathrm{SSA} = \frac{\mathrm{SA}}{4/3\pi r^3 d} \tag{1}$$

where SSA is the specific surface area, SA is the median volume surface area, r is the median volume radius and d is the density of starch, assumed to be constant at 1500 kg/m^3 (Dhital et al., 2010).

2.4. α-Amylase binding assay for the measurement of dissociation constants

Starch binding isotherms were obtained using a modification (Egan, 2008) of published methods (Nielsen et al., 2009; Penninga et al., 1996). A range of starch concentrations from 0.1 to 10 mg/mL was prepared in phosphate buffered saline (PBS, Oxoid Dulbecco A) for each of the different starches. One mL of each starch concentration was transferred to a 1.5 mL microcentrifuge tube. This was cooled to 0 °C on ice for 10 min, before the addition of porcine pancreatic α-amylase (PPA) to give a final concentration of 4 nM (Sigma–Aldrich Chemical Company, order no. 6255) in PBS. The protein concentration of the enzyme preparation was determined by the Bradford reagent assay (Sigma–Aldrich Chemical Company, order no. B6916) and the purity of the enzyme preparation was verified by SDS-PAGE. The concentration was calculated by assuming a relative molecular mass (M_r) of 56 kDa for amylase (Roder et al., 2009; Tahir et al., 2010, 2011). The same concentration of PPA was used for each of the starches investigated. The starch amylase dispersion was left for 30 min at 0 °C to allow the binding of PPA to reach equilibrium, with brief vortexing every 5 min to minimise settling out of granules. The mixture was then spun in a bench top centrifuge for 5 min at 13,400 × g in a cold room at 6 °C. This allowed the separation of all the starch, including bound amylase, from suspension. It was confirmed by optical microscopy (Leitz Dialux 22EB) that all the starch was removed from suspension by the centrifugation step. All binding experiments were carried out at a lowered temperature in order to minimise amylolysis, so that the enzyme binding to starch could be studied in isolation from the hydrolytic phase of the reaction (Fersht, 1999; Nielsen et al., 2009). The reducing sugar concentration in the supernatant was also measured by the Prussian blue reducing assay method (Tahir et al., 2010) and was found not to exceed 50 μM, well below the concentration needed to influence α-amylase behaviour (Seigner, Prodanov, & Marchis-Mouren, 1985). An aliquot of the supernatant (200 μL) containing free (i.e. unbound) enzyme was removed to a fresh microcentrifuge test tube and diluted with 200 μL of PBS. The free enzyme concentration was then determined using an Invitrogen Enzcheck® Ultra α-amylase assay kit, performed according to the manufacturer's instructions. The Enzcheck® assay kit is based on an artificial maize starch substrate, fluorescently labelled to such a high degree that the fluorescence is quenched. This substrate is efficiently degraded by amylase, releasing highly fluorescent fragments. The accompanying increase in fluorescence is proportional to amylase activity and was monitored using a fluorescence microplate reader (BMG Labtech FLUOstar OPTIMA®) at 21 °C. This provided the free enzyme concentration, from which (after taking into account the appropriate assay dilutions) the amount of bound enzyme could be calculated by the following conservation equation:

$$[E]_{\mathrm{bound}} = [E]_0 - [E]_{\mathrm{free}} \tag{2}$$

where $[E]_{\mathrm{bound}}$ is the concentration of bound enzyme, $[E]_0$ is the initial enzyme concentration and $[E]_{\mathrm{free}}$ is the unbound enzyme concentration. Binding constants were obtained by non-linear regression analysis with Enzfitter® software, using a one site binding model:

$$[E]_{\mathrm{bound}} = \frac{B_{\max}[S]}{K_{\mathrm{d}} + [S]} \tag{3}$$

where $B_{\max}$ is the maximum binding capacity, $[S]$ is the starch concentration (mg/mL) and K_{d} is the dissociation constant (mg/mL). These data could also be transformed into a linear plot using the Scatchard equation (Scatchard, 1949):

$$\frac{[E]_{\mathrm{bound}}}{[S]} = \frac{B_{\max}}{K_{\mathrm{d}}} - \frac{[E]_{\mathrm{bound}}}{K_{\mathrm{d}}} \tag{4}$$

If Eq. (4) is obeyed, then a plot of $[E]_{\mathrm{bound}}/[S]$ against $[E]_{\mathrm{bound}}$ will give a straight line with a slope of $1/K_{\mathrm{d}}$ and intercepts of $B_{\max}/K_{\mathrm{d}}$ on the ordinate and $B_{\max}$ on the abscissa.

2.5. α-Amylase binding assay for measurement of binding rates

The rate of α-amylase binding to granular starch was calculated using a modification of the above method. A starch suspension (5 mg/mL in PBS) was prepared, and aliquots of 1 mL were pipetted into a series of 1.5 mL microcentrifuge tubes and placed on ice. At time zero, PPA in PBS was added to each starch sample to give a final PPA concentration of 4 nM. Then at a series of time points from 30 s up to 1 h, tubes containing the starch–enzyme mixture were syringe filtered through a 0.2 μm nylon membrane to rapidly separate the insoluble starch with bound enzyme, from the free, unbound, enzyme. The free enzyme concentration was then determined using the Invitrogen Enzcheck® Ultra α-amylase assay kit, according to the manufacturer's instructions. The bound enzyme concentration was calculated using Eq. (2). The first order binding

rates were then obtained by non-linear regression analysis with the Enzfitter® software, using the following equation:

$$[E]_{\text{bound}} = B_{\max}(1 - \exp^{(-k_{\text{obs}}t)}) \quad (5)$$

where k_{obs} is the observed binding rate constant with dimensions of s^{-1} and t is time in seconds.

Half lives for the binding interaction were calculated from observed binding rate constants using the equation:

$$t_{1/2} = \frac{\ln 2}{k_{\text{obs}}} \quad (6)$$

where $t_{1/2}$ is the half life for the binding interaction in seconds.

To determine the on rate constant, k_{on}, for amylase binding to wheat starch, k_{obs} was determined at a range of enzyme concentrations from 0.4 to 4 nM. This yielded a plot showing a linear relationship between PPA concentration and k_{obs}, which followed the relationship:

$$k_{\text{obs}} = k_{\text{on}}[\text{PPA}] + k_{\text{off}} \quad (7)$$

where k_{on} is the 'on' binding rate constant, k_{off} is the 'off' rate constant and [PPA] is the enzyme concentration. The k_{on} was obtained from the slope of a plot of k_{obs} against enzyme concentration. By extrapolating the k_{obs} values plotted against enzyme concentration to the y-axis intercept, an estimate of k_{off} was also obtained.

2.6. Scanning electron microscopy (SEM)

Images of starches were obtained by dusting the starch onto double-sided sticky tape on an aluminium stub. The samples were uncoated. This was viewed in an FEI Quanta® FEG scanning electron microscope in low vacuum mode, using a 10 keV accelerating voltage. All microscopy experiments were carried out at 21 °C.

2.7. Differential scanning calorimetry (DSC)

All DSC experiments were carried out using a TA instruments Multi-Cell Differential Scanning Calorimeter (MC DSC) with high volume (1 mL) capacity Hallestoy steel ampoules. About 50 mg of starch was accurately weighed into an ampoule and 1.00 g of dH_2O was added. The blank ampoule contained 1.00 g of dH_2O. The samples were scanned from 25 °C to 90 °C at a rate of 0.5 °C min^{-1}, in a chamber constantly purged with nitrogen at a flow rate of 50 mL min^{-1}. The relatively slow heating rate in excess aqueous solution ensures that the gelatinisation process is 'quasi-equilibrium'. All thermograms were analysed using Origin® software to obtain gelatinisation enthalpies as described by Tahir et al. (2010) and Bogracheva, Wang, Wang, and Hedley (2002).

The process of starch gelatinisation is endothermic; heat is taken in by the system in order to break the non-covalent bonding interactions which hold a starch granule together. Crystals have a higher proportion of inter- and intra-molecular non-covalent interactions (e.g. hydrogen bonds, dispersion forces) compared to their disordered, amorphous counterparts. Thus lowering the fraction of crystalline regions present in a material reduces the heat enthalpy required to break open this system, and the enthalpy change associated with gelatinisation can be considered a measure of the relative amounts of crystalline and amorphous material (Craig, Royall, Kett, & Hopton, 1999).

2.8. FTIR–ATR spectroscopy

All FTIR–ATR spectra were collected using a Perkin Elmer Spectrum One® FTIR spectroscope fitted with a SensIR technologies IR II Durascope® diamond cell attenuated total reflectance (ATR) device with a diamond crystal (45° incidence angle). Approximately 5–10 mg of starch was accurately weighed, mixed with an equal mass of dH_2O, and placed on the surface of the ATR device, covered with a 1 cm × 1 cm microscope coverslip. The samples were scanned from 4000 cm^{-1} to 550 cm^{-1}. A total of 26 scans was collected with a resolution of 4 cm^{-1} and co-added for each sample before Fourier transformation. The spectrum for water measured under the same conditions was subtracted from the sample spectra prior to analysis (Capron, Robert, Colonna, Brogly, & Planchot, 2007; Sevenou, Hill, Farhat, & Mitchell, 2002). All measurements were carried out at room temperature (21 °C).

The spectra collected in this study includes the region 1300–800 cm^{-1} of the IR spectra of starch, where there are a number of absorbance bands related to C–C, C–O and C–H stretching, and C–O–H bending modes. Although these bands are yet to be fully assigned, it has been known for some years that the 1022 cm^{-1} absorbance band arises as a result of absorption by stretching modes in amorphous starch, and is therefore sensitive to amorphous structure (van Soest, Tournois, de Wit, & Vliegenthart, 1995). More recently, studies using starches with carefully controlled moisture contents (Capron et al., 2007) have identified the band at 1000 cm^{-1} to result from bonding in hydrated carbohydrate helices. This band is therefore sensitive to organised supramolecular structure, and the ratio of the bands at 1022:1000 cm^{-1} can be used as a measure of the proportion of ordered to amorphous carbohydrate structure in the starch.

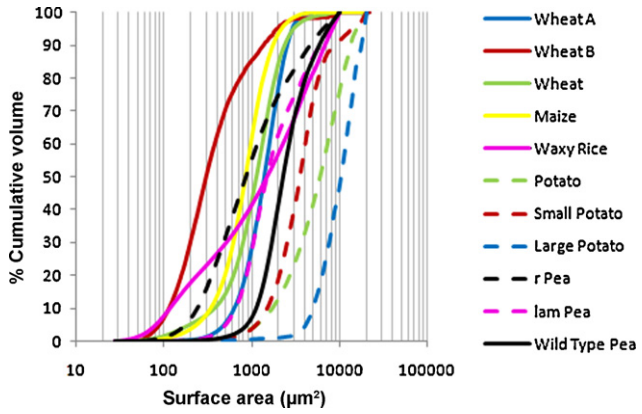

Fig. 1. The particle size distributions of different botanical sources of starch and size fractionated starch granules. Cumulative volume graph showing the distribution of particle size, represented as the cumulative percentage oversize, as measured by the Coulter Counter, and presented as surface area values. The surface area is calculated from the diameter of the starch granules assuming spherical particles.

2.9. Statistical analysis

Pearson correlation and regression analyses were performed between the binding data (K_d and k_{obs}) and the values obtained for surface areas, gelatinisation enthalpies ($\Delta_{\text{gel}}H$, J/g) and FTIR–ATR peak ratio (1022/1000 cm^{-1}) using standard statistical software PASW Statistics 18® (SPSS Inc.®, Chicago, USA). Statistically significant correlations were accepted at $P < 0.05$. Predictions of k_{on} and k_{off} at 95% confidence intervals (CI) were calculated from the linear regression equation of k_{obs} versus PPA concentration, using the slope and intercept coefficients, respectively.

3. Results

3.1. Particle size and surface area analysis

A cumulative oversize plot of all the starches (including size fractions) used in this study is shown in Fig. 1 and the median diameter and specific surface areas are calculated from the distributions (Table 1). It can be seen that the particle size distributions of the

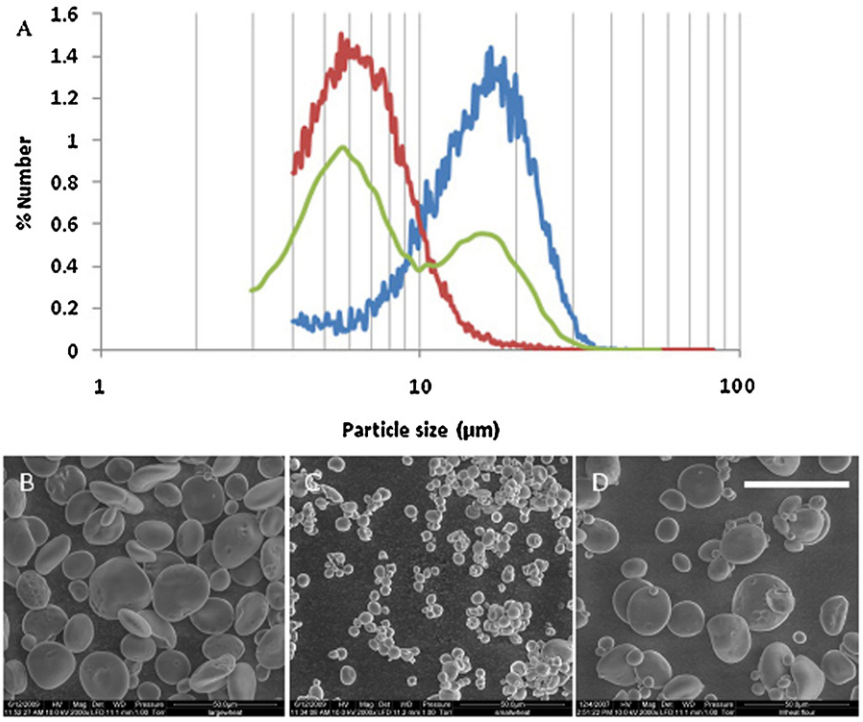

Fig. 2. The particle size distributions (determined by Coulter Counter) of normal and size-fractionated wheat starches with SEM images of each size fraction. Particle size distributions (A) represented as the percentage number of particles in each size bin for wheat starch (green profile) showing a classic biomodal distribution, with large A-type wheat starch granules (blue profile) and small B-type granules (red profile) distributions overlaid, demonstrating the same modal peaks. SEM image B shows fractionated A-type wheat starch. SEM image C shows fractionated B-type wheat starch. SEM image D shows parent wheat starch with large and small granules together. All images were viewed at 2000× magnification with a 10 keV accelerating voltage. The scale bar is 50 μm.

starches cover a very broad range, with median diameters ranging from 9.8 to 60.0 μm, corresponding to median particle surface areas from 0.30 to 11.31 $\times$ 10^3 μm^2, and specific surface areas from 406 to 66 m^2/kg, respectively. It should be noted that starch granule morphology can deviate from perfectly spherical, with some botanical origins of starch granules having polyhederal, flattened or elongated morphologies. The particle volume data initially obtained by the Coulter method is independent of particle size, but to convert this to more useful particle diameter and surface area values, the assumption of perfect sphericity must be made, which may then introduce some small errors.

Wheat starch has a naturally occurring bimodal size distribution, which can be observed in Fig. 2. This distribution was successfully fractionated by density centrifugation into the large (A type) and small (B type) granule fractions, with modal particle sizes that can be seen to match closely the original distribution. Additional evidence that the two distributions were successfully separated is provided by observation with SEM (Fig. 2) which indicates very little contamination of the A type fraction with B type granules, and *vice versa*. There is a large body of literature showing that A and B type wheat starch granule size fractions are very similar in terms of their chemical composition, and other characteristics, such as DSC gelatinisation enthalpy and X-ray diffraction pattern, and differ only in particle size. However, there may be small differences in amylopectin chain length distribution between small and large granules (Ao & Jane, 2007; Kim & Huber, 2010; Salman et al., 2009). In addition to wheat starch, potato starch was also successfully fractionated into two size fractions, with similar characteristics (e.g. similar protein content and degree of starch damage) to the parent starch samples.

Table 1
Particle size parameters for the different botanical sources of native starch and size fractionated starch granules.

Starch type	Median volume diameter[a] (μm)	Median volume surface area[a] (μm^2)	Specific surface area[b] (m^2/kg)
Wheat A	21.1	1400	189
Wheat B	9.8	300	406
Wheat	20.3	1290	190
Maize	17.1	920	233
Waxy rice	22.9	1650	175
Potato	45.2	6420	88
Small potato	35.6	3980	112
Large potato	60.0	11,310	66
r pea	18.0	1020	222
lam pea	22.9	1650	175
Wild type pea	29.1	2670	137

Data analysed according to Tahir et al. (2010).
[a] Median (d_{50}) volume diameters and surface areas calculated from Coulter Counter distributions of particle volume, assuming spherical particles.
[b] Specific surface area calculated from Eq. (1) in Section 2.3.

3.2. Dissociation constants (K_d) for PPA binding to granular starch samples

Using a solution depletion technique (Penninga et al., 1996), the K_d for PPA binding to granular starches at 0 °C was determined for the starches used in this study. For each starch preparation, the enzyme was allowed to equilibrate with the granules for 30 min at 0 °C before centrifugation of the mixture to sediment the starch with its accompanying bound PPA. Determination of the enzyme activity remaining in the supernatant allowed the fraction of bound PPA to be estimated. The binding of amylase to starch was hyperbolic and could be fitted by a typical adsorption isotherm (Fig. 3a). This figure also shows that the data were well fitted by a linear transformation (Scatchard plot) of the binding isotherm using a one-site model. The line to the experimental points was fitted using slope and intercept parameters derived from non-linear fitting of

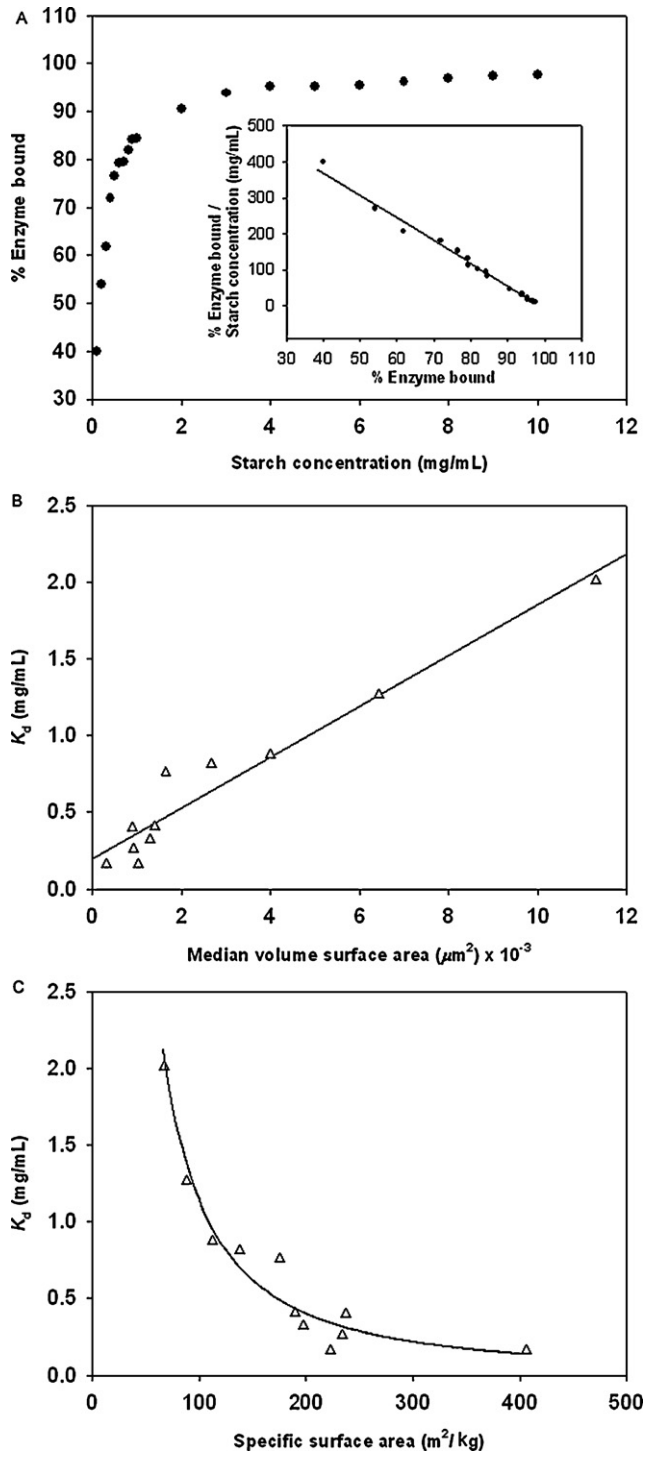

Fig. 3. (a) An example of the enzyme adsorption isotherm for PPA binding to B-type wheat starch granules. A plot of the same data (inset) is fitted to the Scatchard equation (Eq. (4)) with a line derived by using the kinetic parameters (K_d and B_{max}), obtained by non-linear regression of a hyperbolic binding isotherm. (b) The dissociation constant (K_d) values for PPA binding to different botanical sources of starch and size fractionated starch granules plotted against median volume surface area. A strong linear relationship ($R^2 = 0.94$) was found between the starch particle surface area (calculated from median particle diameters) and the dissociation constant for PPA binding to granular starch. (c) The dissociation constant (K_d) values for PPA binding to different botanical sources of starch and size fractionated starch granules plotted against specific surface area. A non-linear relationship was found between starch granule specific surface area and dissociation constant for PPA binding to granular starch. An empirically derived power law relationship was fitted to this data ($R^2 = 0.86$). All experimental points in (a) represent means of duplicate data sets. Experimental points in (b) and (c) represent mean values which were calculated from the regression fitting of duplicate data sets.

Table 2
Dissociation constants (K_d) for PPA binding to different botanical sources of native starch and size fractionated starch granules.

Starch type	K_d (mg/mL)[a]
Wheat A	0.41 ± 0.02
Wheat B	0.16 ± 0.01
Wheat	0.31 ± 0.03
Maize	0.26 ± 0.03
Waxy rice	0.41 ± 0.03
Potato	1.26 ± 0.07
Small potato	0.87 ± 0.08
Large potato	2.05 ± 0.20
r pea	0.17 ± 0.02
lam pea	0.75 ± 0.07
Wild type pea	0.81 ± 0.09

[a] K_d values for PPA binding to each of the starches at 0 °C, presented as mean values ± standard error of the mean (s.e.m.), which were calculated from the non-linear regression fitting of duplicate data sets using Enzfitter® software.

the hyperbolic function (see Section 2.4). The K_d values obtained are shown in Table 2 and it can be seen that these values differed greatly between the different starch samples that were assayed, and also between the separated particle size distributions. Such evidence indicates that particle size, and thus surface area, may be important in determining the affinity of a starch particle towards PPA binding.

As PPA binds to exposed surfaces of a starch granule, which is an insoluble substrate, it is not unexpected perhaps, that the surface area presented by the granule for binding is likely to be an important determinant of apparent binding affinity. When the K_d is plotted against surface area for the starches used in this study, a clear linear relationship ($R^2 = 0.94$) can be seen (Fig. 3b), with larger granule starches having a lower apparent affinity for the enzyme than smaller granules. If the same K_d data are plotted against the specific surface area calculated from the particle size data (Fig. 3c), a lower apparent affinity is observed for PPA binding to starches with a small surface area per unit mass, while granules with a greater surface area per unit mass show a greater apparent affinity for binding the enzyme. This relationship is non-linear however, and the data more easily fits an empirically derived power law ($R^2 = 0.86$).

3.3. Binding rates of PPA binding to granular starch samples

In addition to calculating the K_d at equilibrium, the observed rate constant (k_{obs}) for binding of PPA to starch at 0 °C was determined by using the solution depletion method for mixtures of starch and enzyme that were allowed to interact for accurately determined short periods of time. It was found that PPA binding to insoluble starch at nanomolar concentrations of enzyme is relatively slow and follows first order kinetics with the half life for the binding interaction varying from 30 s up to 6 min (Table 3). Considerable variation between the binding rate constants was observed for different botanical origins of starch. Reports in the literature suggest that amorphous regions of starch granules are hydrolysed more quickly than crystalline regions (Colonna et al., 1992; Gallant, Bouchet, & Baldwin, 1997; Tahir et al., 2010, 2011). We hypothesised that this preference for amorphous starch would be reflected in the binding rate of PPA, with more rapid enzyme binding to relatively disordered amorphous regions of the granule, since such regions are likely to be more accessible than the ordered crystalline regions. Amylose is known to be enriched towards the periphery of the granule (Jane & Shen, 1993), and therefore this linear, amorphous material may favour PPA binding. Also, a run of α-linked glucose residues in an amorphous region would, presumably, be accommodated more favourably within the active site of PPA. The catalytic site of the enzyme contains several sub-sites for glycoside residues and optimal substrate binding is achieved with occupation

Table 3
PPA binding rates (k_{obs}), binding half-life ($t_{1/2}$), gelatinisation enthalpies ($\Delta_{gel}H$) and FTIR–ATR parameters for different botanical sources of native starches.

Starch type	k_{obs}[a] ($\times 10^3\ s^{-1}$)	$t_{1/2}$ (s)	$\Delta_{gel}H$[b] (J/g)	FTIR–ATR peak ratio[c]
Wheat	8.84 ± 0.35	78.4	9.8 ± 0.2	0.98 ± 0.01
Maize	11.90 ± 0.02	49.5	10.7 ± 0.6	0.96 ± 0.01
Waxy rice	1.95 ± 0.07	356.3	15.1 ± 0.7	1.14 ± 0.01
Potato	1.96 ± 0.34	353.0	16.2 ± 0.4	0.87 ± 0.01
r pea	22.04 ± 0.39	31.4	5.3 ± 0.5	1.01 ± 0.01
lam pea	7.75 ± 0.42	89.4	12.4 ± 0.4	0.92 ± 0.02
Wild type pea	6.32 ± 0.39	109.6	11.2 ± 0.2	0.89 ± 0.05

[a] The observed first-order binding rate for PPA binding to granular starch, presented as mean values ± s.e.m., which were calculated from the regression fitting of duplicate data sets and the half-life for the binding interaction calculated from the first order rate.
[b] Gelatinisation enthalpies, calculated from DSC thermograms, for the starches are presented as mean values ± s.e.m. from three determinations.
[c] The ratio of the 1022/1000 cm^{-1} peaks in the FTIR–ATR spectrum of starch are shown as mean values ± s.e.m. from three determinations.

of all the sub-sites (Al Kazaz, Desseaux, Marchis-Mouren, Prodanov, & Santimone, 1998).

It has been shown (Bogracheva et al., 2002) that the gelatinisation enthalpy ($\Delta_{gel}H$) of a starch granule is directly related to the amount of ordered carbohydrate structure in the granule that is disrupted during gelatinisation. The gelatinisation enthalpies for starches used in this study varied from 5.3 J/g to 16.2 J/g (Table 3), indicative of a wide range in the ratio of amorphous to crystalline material. A plot of k_{obs} against $\Delta_{gel}H$ (Fig. 4a) was found to be strongly correlated ($R^2 = 0.87$), showing an inverse linear relationship between enzyme binding rate and gelatinisation enthalpy. Thus, faster enzyme binding was observed for starches with low enthalpies; i.e. those with a more disrupted structure and greater proportion of amorphous content. However, no relationship was found between K_d and $\Delta_{gel}H$ (data not shown).

Another method that can be used to measure the proportion of ordered to disordered α-glucan polymer in starch granules is FTIR–ATR spectroscopy (Capron et al., 2007; Sevenou et al., 2002). This technique is sensitive to changes in conformational order at the surface of the granule. When k_{obs} is plotted against the IR 1022/1000 cm^{-1} peak ratio (Table 3) a linear relationship is observed (Fig. 4b), with higher k_{obs} for enzyme binding to starches with lower peak ratios, which correspond to less ordered structure. There is one anomalous result, however, in that waxy rice starch has an extremely high peak ratio but a relatively low k_{obs} value. This agrees with data obtained by Sevenou et al. (2002) showing that waxy varieties of starch, which are virtually devoid of amylose, produce abnormally high IR peak ratios.

In addition, for wheat starch, a k_{on} value of 1.4 (95% CI: 0.5–2.2) $\times 10^6\ M^{-1}\ s^{-1}$ was determined for PPA binding (Fig. 5), which highlights the relatively slow binding of the enzyme to starch. This value is comparable to that of other tight binding macromolecular interactions involving hydrolytic digestive enzymes (Fersht, 1999). By extrapolation of the linear fit ($R^2 = 0.90$) shown in Fig. 5, where the PPA concentration is zero, k_{off} can also be estimated to be around 2.6 (95% CI: 0.4–4.9) $\times 10^{-3}\ s^{-1}$, which would indicate a K_d for enzyme binding of approximately 2 nM, as calculated from the ratio of k_{off} and k_{on}.

4. Discussion

In a previous paper (Tahir et al., 2010), we showed that the kinetic parameters (e.g. K_m, the Michaelis–Menten constant) of the initial rates (within the first 10 min) of starch hydrolysis by PPA were related to physical parameters of the starch granule in a complex manner. The work presented in this paper helps to clarify the effects of different physical characteristics of starch on its susceptibility to hydrolysis by PPA, by looking at the kinetically important step (Slaughter et al., 2001) of the enzyme binding to the starch granule, independently of subsequent hydrolysis. We have shown for the first time that the binding kinetics of PPA to starch is strongly dependent on the physical characteristics of the granule. We cannot rule out the potential role of non-carbohydrate components of starch (e.g. lipid, protein) in modifying this process, but we believe that this effect is likely to be minor, in comparison to the importance of the physical structure of the carbohydrate.

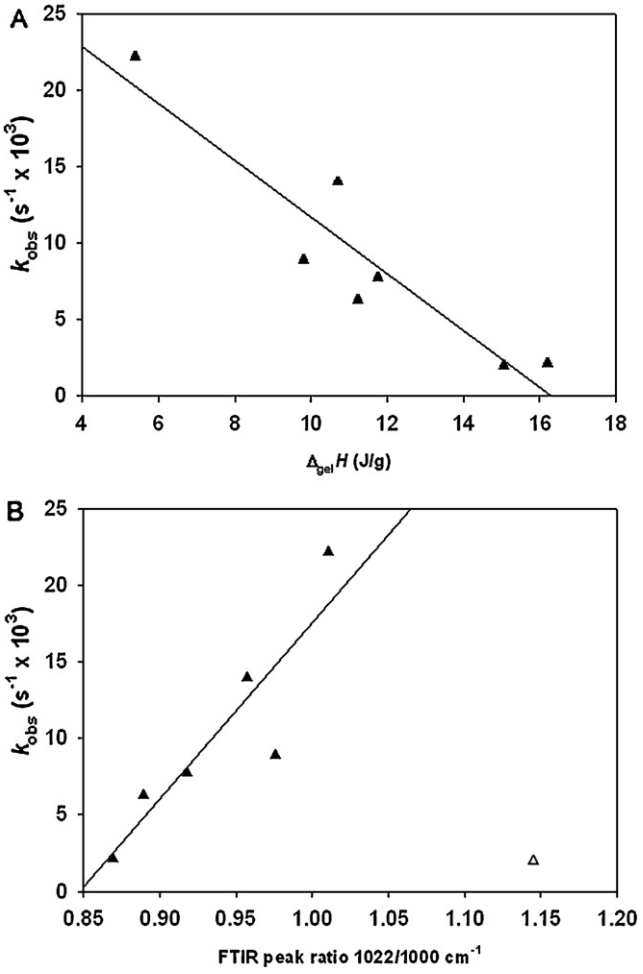

Fig. 4. (a) Gelatinisation enthalpies ($\Delta_{gel}H$) for different botanical sources of starch plotted against their observed binding rate (k_{obs}) for PPA. A strong linear inverse relationship ($R^2 = 0.87$) was found between starch gelatinisation enthalpies, as measured by DSC, and the observed first-order binding rate constant. (b) The FTIR–ATR peak ratio (1022/1000 cm^{-1}) for different botanical sources of starches plotted against their observed binding rate (k_{obs}) for PPA. A linear relationship ($R^2 = 0.80$) was found between the ratio of the FTIR–ATR spectrum peaks at 1022 cm^{-1} and 1000 cm^{-1}, and the observed first order binding rate constant. One anomalous point (△) was observed for the waxy rice starch. All experimental points in (a) and (b) represent mean values which were calculated from the regression fitting of duplicate data sets.

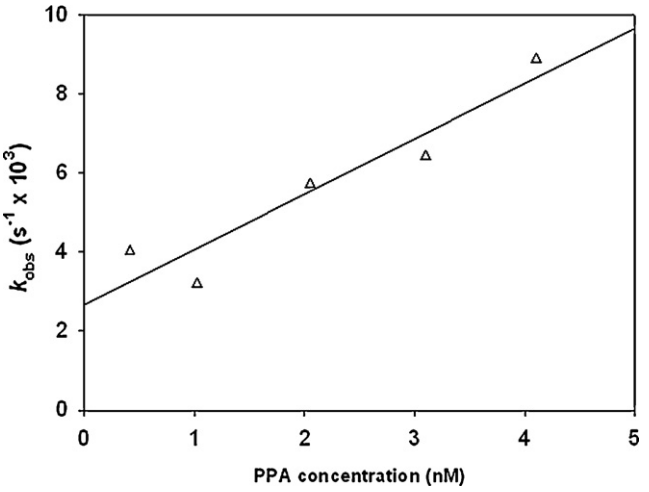

Fig. 5. The observed binding rate (k_{obs}) values for PPA binding to wheat starch plotted against PPA concentration. The k_{obs} values for PPA binding to wheat starch determined at a range of enzyme concentrations, fitted with a linear regression ($R^2 = 0.90$). The on rate (k_{on}) value is equal to the slope of the regression fit with units of $M^{-1}\ s^{-1}$, and the off rate (k_{off}) is estimated from extrapolating the fit to its intercept on the y-axis, where PPA concentration is zero, with units of s^{-1}. The linear regression equation is as follows: $y = 1.4$ (s.e. 0.3) $x + 2.6$ (s.e. 0.7), where $y = k_{obs}$ ($\times 10^3\ s^{-1}$) and x = PPA concentration (nM). The intercept and slope coefficients (shown with respective standard errors, s.e.) for the linear regression model were highly significant ($P < 0.03$ and <0.01, respectively).

The K_d values obtained in this study indicate the availability of starch for enzyme binding at equilibrium for different botanical origins of starch. The dissociation constants show a clear relationship with the particle size, indicating that the surface area to volume ratio of the starch granule is a very important factor in determining the area of exposed carbohydrate available for enzyme binding, and a reflection of the number of available α-glucan chains. This result may go some way to explain why certain groups of investigators have observed strong particle size effects on the hydrolysis of starch granules, whereas others have failed to demonstrate any such effect (Tahir et al., 2010). Starch hydrolysis experiments performed on a number of different starches for comparison purposes have usually been carried out with reaction mixtures containing a very high, fixed enzyme concentration plus the test starches at the same concentration irrespective of source (Dhital et al., 2010; Knutson et al., 1982; Manelius et al., 1997; Planchot et al., 1995; Sakintuna, Budak, Dik, Yondem-Makascioglu, & Kincal, 2003; Valetudie et al., 1993; Vasanthan & Bhatty, 1996). These previous hydrolysis experiments were performed using estimated enzyme concentrations of between 100 and 500 nM, while amylase concentrations in the lumen of the human gut have been estimated to range from 5 to 15 nM (Slaughter et al., 2001). Whether any effect of particle size will be seen in such studies depends on the particular experimental conditions that are selected. Very high enzyme concentrations may overcome the relative disadvantages associated with a larger surface area, because the high concentration is likely to drive the system to the saturation of all available binding sites, even if the latter possess relatively poor affinities. Under these conditions, detection of any differences in affinities associated with particle size could be difficult. Thus, the only study designs that can reliably demonstrate a role for particle size in starch hydrolysis rates are those that observe the kinetic parameters for the initial rates of hydrolysis over a range of starch concentrations (Byoung-Wook et al., 2003; Tahir et al., 2010, 2011).

Our previous studies (Tahir et al., 2010) show a clear association between starch granule surface area and K_m, a parameter that can be considered to indicate the amount of α-glucan chains on the granule surface available for enzyme binding. Similarly, a relationship between surface area and K_d is therefore also to be expected. At starch concentrations close to the K_m value, a strong relationship is also seen between hydrolysis rate and particle size (Tahir et al., 2010). Our previous paper (Tahir et al., 2010) reports a very similar relationship between specific surface area and K_m to that which we now report for specific surface area and K_d. These findings present strong evidence for the conclusion that for starch interacting with PPA both the experimentally determined K_m and K_d values underline the importance of available surface area per unit weight.

The rate constant for adsorption of enzyme onto the surface of the granule was also measured in the present study. Because starch is a large, granular substrate it is not surprising that the enzyme binds relatively slowly to granule surfaces, with a half life for the binding interaction, at nM concentrations of enzyme, which ranges from 30 s to 6 min between the different starches that were assayed. An on rate of $1.4 \times 10^6\ M^{-1}\ s^{-1}$ for enzyme binding to wheat starch underlines how slow this binding is, and how kinetically important it is, taking into consideration that the k_{cat} for native wheat starch hydrolysis by PPA is approximately $2 \times 10^4\ s^{-1}$ (Tahir et al., 2010, 2011). Assuming that the difference between k_{on} and k_{cat} indicates the rate of the hydrolysis step itself, this would suggest a rate of $\sim 10^2\ s^{-1}$ with a kinetically relevant binding step.

The initial rates of hydrolysis of semi-crystalline carbohydrate substrates such as starch (Tahir et al., 2011) and microcrystalline cellulose (Hall, Bansal, Lee, Realff, & Bommarius, 2010) have been shown to be dependent on the ratio of ordered to disordered glucan polymer, with slower hydrolysis rates from substrates with a greater proportion of ordered material. Slaughter et al. (2001) demonstrated that the adsorption of enzyme to the surface of the starch granule is a kinetically important step in the hydrolysis of native starch granules, and this may be inversely related to the fraction of crystalline material in the granule. The binding rate data presented in this paper show a significant relationship with two parameters that provide a measure of the degree of ordered starch granular structure, namely DSC and IR spectroscopy. DSC provides a measure of the bulk crystallinity of a starch granule, which in aqueous suspension represents the majority of the ordered material in the granule (Bogracheva et al., 2002). The observed rate constant for PPA binding to granules is highest for those with a large amorphous content, while an increase in crystalline content decreases the rate constant for enzyme binding. This indicates that the enzyme preferentially binds to amorphous material, although the lack of any relationship between K_d data and $\Delta_{gel}H$ suggests that at equilibrium, the enzyme may bind to both ordered and amorphous material.

FTIR–ATR has been shown to be insensitive to long range crystalline ordering, and the crystalline subtype, of the starch granule. Instead, FTIR–ATR provides a measure indicating the amount of short range carbohydrate structuring. It is a surface specific technique, because the IR beam only penetrates to a depth of 2 μm at the wavelengths used in studies of starch structure (see the work of Capron et al., 2007; Sevenou et al., 2002 for a full discussion of the usefulness of the technique). When the IR peak ratios are compared to the enzyme binding rates, the same trend is seen as with the DSC data, i.e., with higher k_{obs} values for the enzyme binding to those starches containing the most disordered material, and slower binding to starches with higher amounts of ordered carbohydrate. Taken together, the DSC and FTIR–ATR results demonstrate that PPA binds preferentially to disordered, amorphous material, which means that there is potentially faster enzyme binding to granules with a greater amorphous content. Interestingly, this result suggests that the ratio of ordered-disordered material at the granule surface (as measured by FTIR–ATR) is broadly similar to the bulk (as measured by DSC) in its influence on PPA binding. Our novel finding that the enzyme preferentially binds to starches with a greater frac-

tion of amorphous material is consistent with conclusions drawn from our recent enzyme kinetic studies (Tahir et al., 2010, 2011).

5. Conclusions

The data presented in this paper focus on the initial binding interaction between granular starch, a complex, semi-crystalline substrate, and an important hydrolytic enzyme, α-amylase. We have shown that at equilibrium, the amount of enzyme bound to the starch granule surface is dependent on the particle size and therefore the surface area of the starch granule. Prior to reaching equilibrium, the rate of the kinetically important slow binding step of the enzyme to the surface of the granule is related to the degree of carbohydrate order at the surface of the granule. Thus, granules with a higher proportion of amorphous material are more accessible to the enzyme and thus allow it to bind faster. We consider that the information gained from these studies of amylase binding to starch, i.e., the first stage in the catalytic reaction, is likely to be of relevance in industrial applications of amylase action and in understanding initial stages in the biochemistry of mammalian starch digestion.

Acknowledgments

We thank Mr Steve Ingham for assistance with particle sizing, Dr. Anthony Brain for assisting with scanning electron microscopy, Dr Ram Abuknesha and Dr Dirk Wildeboer for assistance with the fluorimetry and Dr Danielle Egan for suggesting the use of solution depletion assays. Mr Peter Milligan provided expert advice on statistical analyses of data. FJW was supported by a Kings College London scholarship.

References

Ao, Z., & Jane, J. L. (2007). Characterization and modeling of the A- and B-granule starches of wheat, triticale, and barley. *Carbohydrate Polymers*, *67*, 46–55.

Al Kazaz, M., Desseaux, V., Marchis-Mouren, G., Prodanov, E., & Santimone, M. (1998). The mechanism of porcine pancreatic α-amylase – inhibition of maltopentaose hydrolysis by acarbose, maltose and maltotriose. *European Journal of Biochemistry*, *252*, 100–107.

Bogracheva, T. Y., Wang, Y. L., Wang, T. Y., & Hedley, C. L. (2002). Structural studies of starches with different water contents. *Biopolymers*, *64*, 268–281.

Boistelle, R., Astier, J. P., Marchis-Mouren, G., Desseaux, V., & Haser, R. J. (1992). Solubility, phase transition, kinetic ripening and growth rates of porcine pancreatic α-amylase isoenzymes. *Journal of Crystal Growth*, *123*, 109–120.

Butterworth, P. J., Ellis, P. R., & Roder, N. (2005). Starch molecular and nutritional properties: A review. *Advances in Molecular Medicine*, *1*, 5–14.

Byoung-Wook, K., Jung-In, K., Myo-Jeong, K., & Jae, C. K. (2003). Porcine pancreatic α-amylase hydrolysis of native starch granules as a function of granule surface area. *Biotechnology Progress*, *19*, 1162–1166.

Capron, I., Robert, P., Colonna, P., Brogly, M., & Planchot, V. M. (2007). Starch in rubbery and glassy states by FTIR spectroscopy. *Carbohydrate Polymers*, *68*, 249–259.

Colonna, P., Leloup, V. M., & Buleon, A. (1992). Limiting factors of starch hydrolysis. *European Journal of Clinical Nutrition*, *46*, S17–S32.

Craig, D. Q. M., Royall, P. G., Kett, V. L., & Hopton, M. L. (1999). The relevance of the amorphous state to pharmaceutical dosage forms: Glassy drugs and freeze dried systems. *International Journal of Pharmacuetics*, *179*, 179–207.

Dhital, S., Shrestha, A. K., & Gidley, M. J. (2010). Relationship between granule size and in vitro digestibility of maize and potato starches. *Carbohydrate Polymers*, *82*, 480–488.

Egan, D. (2008). *The biochemical mechanism of starch digestion: Enzyme kinetic studies of alpha-amylase action on starch*. Ph.D. thesis, King's College London, UK.

Ells, L. J., Seal, C. J., Kettlitz, B., Bal, W., & Mathers, J. C. (2005). Postprandial glycaemic, lipaemic and haemostatic responses to ingestion of rapidly and slowly digested starches in healthy young women. *British Journal of Nutrition*, *94*, 948–955.

Fersht, A. (1999). Measurement and magnitude of individual rate constants. In *Structure and mechanism in protein science*. New York, USA: Freeman., pp. 132–168.

Gallant, D. J., Bouchet, B., & Baldwin, P. M. (1997). Microscopy of starch: Evidence of a new level of granule organization. *Carbohydrate Polymers*, *32*, 177–191.

Hall, M., Bansal, P., Lee, J. H., Realff, M. J., & Bommarius, A. S. (2010). Cellulose crystallinity—A key predictor of the enzymatic hydrolysis rate. *FEBS Journal*, *277*, 1571–1582.

Jane, J.-L., & Shen, J. J. (1993). Internal structure of the potato starch granule revealed by chemical gelatinization. *Carbohydrate Research*, *247*, 279–290.

Kim, H. S., & Huber, K. C. J. (2010). Physicochemical properties and amylopectin fine structures of A- and B-type granules of waxy and normal soft wheat starch. *Cereal Science*, *51*, 256–264.

Kim, H. S., & Huber, K. C. (2008). Channels within soft wheat starch A- and B-type granules. *Journal of Cereal Science*, *48*, 159–172.

Knutson, C. A., Khoo, U., Cluskey, J. E., & Inglett, G. E. (1982). Variation in enzyme digestibility and gelatinization behavior of corn starch granule fractions. *Cereal Chemistry*, *59*, 512–515.

Leloup, V. M., Colonna, P., & Ring, S. G. (1991). α-Amylase adsorption on starch crystallites. *Biotechnology and Bioengineering*, *38*, 127–134.

Lloyd, J. R., Hedley, C. L., Bull, V. J., & Ring, S. G. (1996). Determination of the effect of r and rb mutations on the structure of amylose and amylopectin in pea (*Pisum sativum* L.). *Carbohydrate Polymers*, *29*, 45–49.

MacGregor, A. W. (1979). Isolation of large and small granules of barley starch and a study of factors influencing the adsorption of barley malt α-amylase by these granules. *Cereal Chemistry*, *56*, 430–434.

Manelius, R., Qin, Z., Åvall, A.-K., Andtfolk, M., & Bertoft, E. (1997). The mode of action on granular wheat starch by bacterial α-amylase. *Starch-Stärke*, *49*, 142–147.

Mann, J. (2007). Dietary carbohydrate: Relationship to cardiovascular disease and disorders of carbohydrate metabolism. *European Journal of Clinical Nutrition*, *61*(Suppl. 1), S100–S111.

Mclaren, A. D. (1963). Enzyme reactions in structurally restricted systems. IV. The digestion of insoluble substrates by hydrolytic enzymes. *Enzymologia*, *26*, 237–246.

Nielsen, M. M., Bozonnet, S., Seo, E. S., Móytán, J. A., Andersen, J. M., Dilokpimol, A., et al. (2009). Two secondary carbohydrate binding sites on the surface of barley α-amylase 1 have distinct functions and display synergy in hydrolysis of starch granules. *Biochemistry*, *48*, 7686–7697.

Penninga, D., van der Veen, B. A., Knegtel, R. M. A., van Hijum, S. A. F. T., Rozeboom, H. t. J., Kalk, K. H., et al. (1996). The raw starch binding domain of cyclodextrin glycosyltransferase from *Bacillus circulans* strain 251. *Journal of Biological Chemistry*, *271*, 32777–32784.

Planchot, V., Colonna, P., Gallant, D. J., & Bouchet, B. J. (1995). Extensive degradation of native starch granules by α-amylase from *Aspergillus fumigatus*. *Journal of Cereal Science*, *21*, 163–171.

Robertson, G. H., Wong, D. W. S., Lee, C. C., Wagschal, K., Smith, M. R., & Orts, W. J. (2005). Native or raw starch digestion: A key step in energy efficient biorefining of grain. *Journal of Agricultural and Food Chemistry*, *54*, 353–365.

Robyt, J. F. (2008). Starch: Structure, properties, chemistry, and enzymology. In B. Fraser-Reid, K. Tatsuta, & J. Thiem (Eds.), *Glycoscience* (pp. 1438–1472). Berlin, Germany: Springer.

Roder, N., Gerard, C., Verel, A., Bogracheva, T. Y., Hedley, C. L., Ellis, P. R., et al. (2009). Factors affecting the action of α-amylase on wheat starch: Effects of water availability. An enzymic and structural study. *Food Chemistry*, *113*, 471–478.

Sakintuna, B., Budak, O., Dik, T., Yondem-Makascioglu, F., & Kincal, N. S. (2003). Hydrolysis of freshly prepared wheat starch fractions and commercial wheat starch using α-amylase. *Chemical Engineering Communications*, *190*, 883–897.

Salman, H., Blazek, J., Lopez-Rubio, A., Gilbert, E. P., Hanley, T., & Copeland, L. (2009). Structure–function relationships in A and B granules from wheat starches of similar amylose content. *Carbohydrate Polymers*, *75*, 420–427.

Scatchard, G. (1949). The attractions of proteins for small molecules and ions. *Annals of the New York Acadamy of Sciences*, *51*, 660–672.

Schwimmer, S., & Balls, A. K. (1949). Starches and their derivatives as adsorbents for malt α-amylase. *Journal of Biological Chemistry*, *180*, 883–894.

Seigner, C., Prodanov, E., & Marchis-Mouren, G. (1985). On porcine pancreatic α-amylase action: Kinetic evidence for the binding of two maltooligosaccharide molecules (maltose, maltotriose and *o*-nitrophenylmaltoside) by inhibition studies. *European Journal of Biochemistry*, *148*, 161–168.

Sevenou, O., Hill, S. E., Farhat, I. A., & Mitchell, J. R. (2002). Organisation of the external region of the starch granule as determined by infrared spectroscopy. *International Journal of Biological Macromolecules*, *31*, 79–85.

Slaughter, S. L., Ellis, P. R., & Butterworth, P. J. (2001). An investigation of the action of porcine pancreatic α-amylase on native and gelatinised starches. *Biochimica et Biophysica Acta – General Subjects*, *1525*, 29–36.

Svihus, B., Uhlen, A. K., & Harstad, O. M. (2005). Effect of starch granule structure, associated components and processing on nutritive value of cereal starch: A review. *Animal Feed Science and Technology*, *122*, 303–320.

Tahir, R., Ellis, P. R., & Butterworth, P. J. (2010). The relation of physical properties of native starch granules to the kinetics of amylolysis catalysed by porcine pancreatic α-amylase. *Carbohydrate Polymers*, *81*, 57–62.

Tahir, R., Ellis, P. R., Bogracheva, T. Y., Meares-Taylor, C., & Butterworth, P. J. (2011). Study of the structure and properties of native and hydrothermally processed wild-type, *lam* and *r* variant pea starches that affect amylolysis of these starches. *Biomacromolecules*, *12*, 123–133.

Tan, I., Flanagan, B. M., Halley, P. J., Whittaker, A. K., & Gidley, M. J. (2007). A method for estimating the nature and relative proportions of amorphous, single, and double-helical components in starch granules by ^{13}C CP/MAS NMR. *Biomacromolecules*, *8*, 885–891.

Tester, R. F., Qi, X., & Karkalas, J. (2006). Hydrolysis of native starches with amylases. *Animal Feed Science and Technology*, *130*, 39–54.

Valetudie, J.-C., Colonna, P., Bouchet, B., & Gallant, D. J. (1993). Hydrolysis of tropical tuber starches by bacterial and pancreatic α-amylases. *Starch-Stärke*, *45*, 270–276.

van Soest, J. J. G., Tournois, H., de Wit, D., & Vliegenthart, J. F. G. (1995). Short-range structure in (partially) crystalline potato starch determined with attenuated

total reflectance Fourier-transform IR spectroscopy. *Carbohydrate Research*, *279*, 201–214.

Vasanthan, T., & Bhatty, R. S. (1996). Physicochemical properties of small- and large-granule starches of waxy, regular, and high-amylose barleys. *Cereal Chemistry*, *73*, 199–207.

Wang, T. L., Bogracheva, T. Y., & Hedley, C. L. (1998). Starch: As simple as A, B, C? *Journal of Experimental Botany*, *49*, 481–502.

Zhang, T., & Oates, C. G. (1999). Relationship between α-amylase degradation and physico-chemical properties of sweet potato starches. *Food Chemistry*, *65*, 157–163.